

NYS College of Ceramics @ A.U. ILL

Borrower: COO

Call #: TJ260 H395 1984

ILLiad TN: 88251



COO

Lending String:

Location:

ARIEL

ODYSSEY ENABLED

Patron:

Journal Title: AIChE symposium series.

Charge

Volume 80 236

Maxcost: 10.00IFM

Volume: 104 **Issue:** 4

Month/Year: 1984 **Pages:** 65-75

Article Author: *69-75*
Suresh - Avedisian?

Article Title: Heat Transfer Controlled Bubble
Growth in a Superheated Liquid Droplet?

Shipping Address:

COO - CORNELL UNIVERSITY
Olin Library - Interlibrary Services
Central Avenue
Ithaca, NY 14853-5301

Odyssey

Fax: Please do not s

Article exchange 128.253.78.96

Email: mann_ill@cornell.edu

ILL Number: 145617628



*** If this is not the article you are looking please resubmit with additional info. Thanks ***

HEAT TRANSFER CONTROLLED BUBBLE GROWTH IN A SUPERHEATED LIQUID DROPLET

K. Suresh and C.T. Avedisian ■

Sibley School of Mechanical and Aerospace Engineering, Cornell University, Ithaca, NY 14853

Bubble growth within a volatile superheated liquid droplet (liquid1) vaporizing in a hot nonvolatile immiscible liquid (liquid2) is analyzed by solving the coupled energy equations for the temperature fields in liquids 1 and 2. A numerical solution of the governing equations was obtained for a two phase droplet modelled as a vapor bubble growing from the center of liquid1. It is shown that when the physical properties of liquids 1 and 2 are appreciably different, the droplet vaporization rate can be dramatically increased or decreased when the thermal boundary layer extends into liquid2.

INTRODUCTION

Previous work on bubble growth within liquid droplets has focussed on the effect of the droplet on the flow and heat transfer processes in the external field liquid [1-5]. Concomitant processes within the droplet interior were neglected. The present work takes into account the effect of the velocity and temperature fields both within and exterior to the droplet on the temporal variation of the bubble and droplet radii.

FORMULATION

We consider a single stationary spherical droplet of initial radius S_0 of the vaporizing liquid (liquid1) suspended in a stagnant field liquid (liquid2) of infinite extent. We assume (1) the two liquids are mutually immiscible, (2) the pressure is everywhere uniform at P_0 (dynamic effects are thus absent), (3) the entire system is initially at a temperature T_0 which corresponds to the homogeneous nucleation temperature of liquid1 at P_0 , (4) viscous effects are negligible, and (5) all thermophysical properties are constant.

At time $t=0$ a vapor bubble is formed spontaneously by homogeneous nucleation at the center of the droplet (see Figure 1). Experimental evidence [1,6] has shown that when as little as 10% of the mass of organic liquid droplets has vaporized, and the liquid

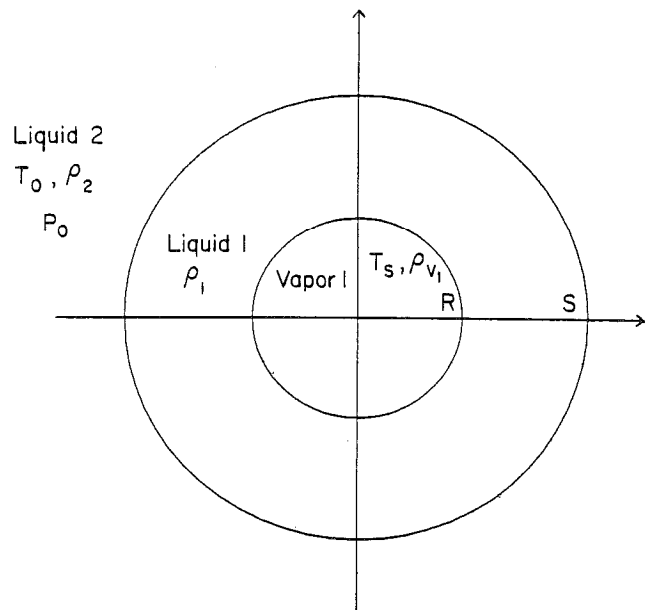


Fig. 1. Geometry of the proposed model.

to vapor density ratio is large enough ($T_r \leq .95$), liquid surrounding the droplet essentially exists in the form of a thin film. In this event any effects of eccentricity of the vapor bubble on its growth rate will be minimal. The temperature within the vapor bubble is assumed to be uniform and equal to the saturation temperature, T_s , of liquid1 at pressure P_0 . The temperature difference between the vapor and the ambient liquid phase causes a flow of energy into the bubble. This energy provides the heat to

vaporize the droplet, and the bubble then begins to grow.

GOVERNING EQUATIONS

The temperature field in the two liquid phases is governed by the following form of the energy equation [7]:

$$\frac{\partial T_i}{\partial t} = \alpha_i \frac{1}{r^2} \frac{\partial}{\partial r} \left(r^2 \frac{\partial T_i}{\partial r} \right) - \frac{\epsilon \dot{R} R^2}{r^2} \frac{\partial T_i}{\partial r} \quad (1)$$

where $i=1$ for $R < r < S$, and $i=2$ for $S < r < \infty$.

The boundary and initial conditions to complete the formulation of the problem are the following:

$$T_1(0, r) = T_2(0, r) = T_0 \quad (2)$$

$$T_1(R, t) = T_s \quad (3)$$

$$T_1(S, t) = T_2(S, t) \quad (4)$$

$$k_1 \left. \frac{\partial T_1}{\partial r} \right|_{r=S} = k_2 \left. \frac{\partial T_2}{\partial r} \right|_{r=S} \quad (5)$$

$$T_2(\infty, t) = T_0 \quad (6)$$

where T_0 is the limit of superheat of liquid1 at the pressure P_0 (e.g., [8]).

In the present model, the growth of the bubble is completely controlled by the rate of heat transfer to the vapor/liquid1 interface. A heat balance at this surface yields:

$$k_1 \left. \frac{\partial T_1}{\partial r} \right|_{r=R} = \rho_v h_{fg} \dot{R} \quad (7)$$

METHOD OF SOLUTION

We adopt a coordinate transformation similar to the one suggested by Duda et al. [9], generalized by Saitoh [10], and subsequently used in connection with melting and freezing problems [11-13]. This transformation immobilizes the boundaries at fixed coordinate values in the transformed space. The variable transformation is

$$\eta = \frac{r-R(t)}{S(t)-R(t)}, \quad \tau = \bar{t} \quad (8)$$

Eq. 9 fixes the two moving boundaries at $\eta=0$ (vapor1/liquid1 interface) and $\eta=1$ (liquid1/liquid2 interface).

The following non-dimensional quantities are now introduced

$$\bar{T} = \frac{T-T_s}{T_0-T_s} \quad \bar{r} = \frac{r}{S_0} \quad R = \frac{\bar{R}}{S_0} \quad \dot{\bar{R}} = \frac{\dot{R} S_0}{\alpha_1} \\ \bar{t} = \frac{t \alpha_1}{S_0^2} \quad \gamma = \alpha_2/\alpha_1 \quad \zeta = k_2/k_1 \quad (9)$$

Together with the co-ordinate transformation (Eq. 9), the energy equation becomes:

$$A_i(\eta, \tau) \frac{\partial \bar{T}_i}{\partial \tau} = \frac{\partial}{\partial \eta} \left[B_i(\eta, \tau) \frac{\partial \bar{T}_i}{\partial \eta} \right] - D_i(\eta, \tau) \frac{\partial \bar{T}_i}{\partial \eta} \quad (10)$$

with

$$A_i(\eta, \tau) = \bar{r}^2 (\bar{S} - \bar{R}) / d_i$$

$$B_i(\eta, \tau) = \bar{r}^2 / (\bar{S} - \bar{R})$$

$$D_i(\eta, \tau) = \left[\epsilon \bar{R}^2 + \frac{\bar{r}^3 (\bar{S}^2 - \epsilon \bar{R}^2) - \bar{r}^2}{\bar{S}^2 (\bar{S} - \bar{R})^2} \right] \dot{\bar{R}} / d_i \quad (11)$$

where $i=1,2$, $d_1=1$ ($0 \leq \eta < 1$),
 $d_2=\gamma$ ($0 \leq \eta < \infty$),

and $r = \eta(\bar{S} - \bar{R}) + \bar{R}$

The transformed initial and boundary conditions are:

$$\bar{T}_1(\eta, 0) = \bar{T}_2(\eta, 0) = 1 \quad (12)$$

$$\bar{T}_1(0, \tau) = 0 \quad (13)$$

$$\bar{T}_1(1, \tau) = \bar{T}_2(1, \tau) \quad (14)$$

$$\left. \frac{\partial \bar{T}_1}{\partial \eta} \right|_{\eta=1} = \zeta \left. \frac{\partial \bar{T}_2}{\partial \eta} \right|_{\eta=1} \quad (15)$$

$$\bar{T}_2(\infty, \tau) = 1 \quad (16)$$

Finally, the interface heat balance is transformed to

$$\dot{\bar{R}} = \frac{Ja}{(\bar{S} - \bar{R})} \left. \frac{\partial \bar{T}_1}{\partial \eta} \right|_{\eta=0} \quad (17)$$

where Ja is the Jakob number defined by

$$Ja = \frac{C_{p1}(T_o - T_s)\rho_1}{\rho_v h_{fg}} \quad (18)$$

Four non-dimensional groups control the radius-time history of the bubble: Ja, ε, γ, ζ.

The coupled energy equations for liquid1 and liquid2 were solved simultaneously by finite difference methods. A Crank-Nicholson method was used to simultaneously integrate the energy equation (Eq. 10) and the interface equation (Eq. 17) at each time-step to obtain the temperature field and the bubble radius as functions of time.

The droplet radius was then obtained from the bubble radius by a mass balance as

$$\bar{S} = (1 + \epsilon \bar{R}^3)^{1/3} \quad (19)$$

Further details of the numerical procedure may be found in [14].

Bubble growth is assumed to stop when liquid1 is completely vaporized. At this time the radius of the bubble (and "droplet") is then given by

$$\bar{R}_f = (1 - \epsilon)^{-1/3} \quad (20)$$

RESULTS AND DISCUSSIONS

Calculations were performed for a variety of combinations of the four parameters Ja, ε, γ and ζ. Most liquids of interest have ε very close to 1 for reduced temperatures of interest and all calculations presented here are therefore for ε→1. The ranges of variation of the other parameters were chosen to correspond to properties typical of hydrocarbon-glycerine and hydrocarbon-water combinations.

Figures 2 and 3 show bubble radius as a function of time for Ja = 10 and ε = 0.995 with either γ (Fig. 2) or ζ (Fig. 3) as a parameter. The most significant feature of the results shown in these figures is that all curves are identical up to some particular time (τ=0.01) and then differ beyond this time. This result can be explained using the concept of a thermal boundary layer which surrounds the bubble, and within which the temperature changes from T_s to T_o. The temperature field outside this boundary layer is almost unperturbed from the initial condition. As the bubble grows, the thermal boundary layer propagates outward from the

liquid1/vapor interface, approaches the liquid1/liquid2 interface, and then

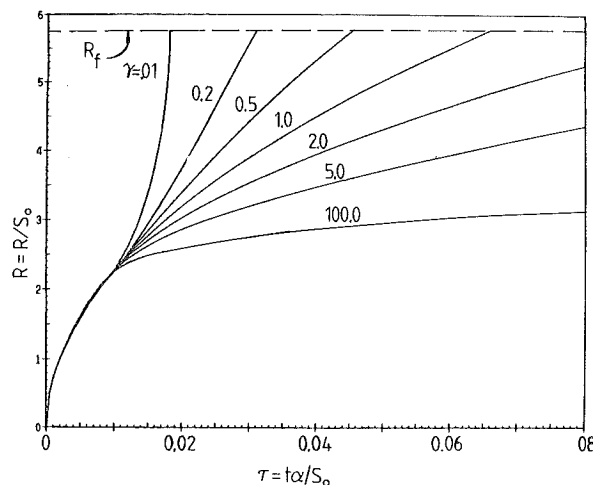


Fig. 2. Temporal variation of bubble radius with time illustrating the effect of γ(ζ=1) for Ja=10, ε=0.995

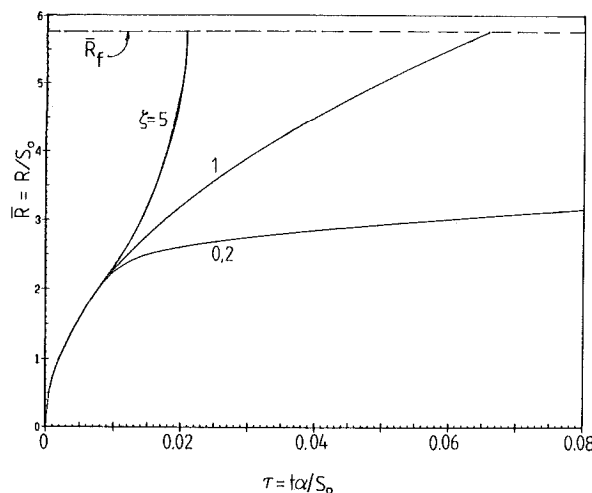


Fig. 3. Temporal variation of bubble radius with time illustrating the effect of ζ(γ=1) for Ja=10 and ε=0.995.

penetrates into liquid2. Before this penetration occurs, the field liquid has no effect on bubble growth since its temperature remains at the initial value, and the bubble grows in a manner identical to its growth in an infinite medium of liquid1. Previous analyses for bubble growth in an infinite medium (e.g., [7]) may thus be applied to describe bubble growth in the finite medium of the liquid droplet during this initial period. Only when the thermal boundary layer penetrates into liquid2 do field liquid properties, and hence the finite mass of the va-

porizing liquid, affect the heat transfer and bubble growth rates. This fact is reflected in the various growth curves which fan out as shown in Figures 2 and 3.

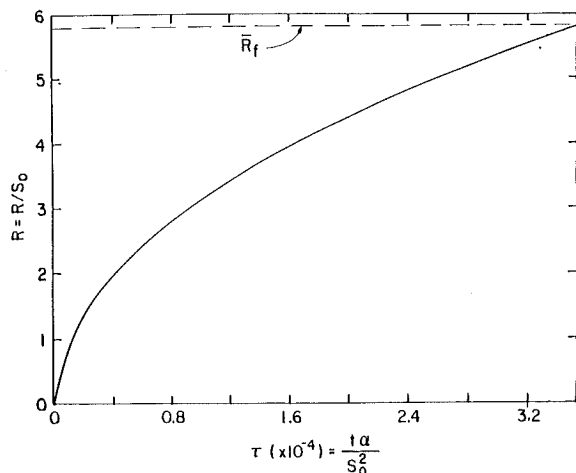


Fig. 4. Temporal variation of bubble radius for $Ja=100$ and $\epsilon=.995$. All ranges of γ and ζ .

For $Ja=100$, Fig. 4 reveals that the thermal boundary layer remains entirely within the droplet throughout vaporization of liquid1 since the properties of liquid2 do not affect growth. This qualitatively supports an earlier simplified model [6] for bubble growth within a liquid droplet at high superheats. The unique growth curve in Fig. 4 is therefore identical to vapor bubble growth in an infinite medium of liquid1. In addition, as Jakob number increases the bubble grows faster (compare the time scales in Figures 2-4) as would be expected due to increased heat transfer to the bubble attendant to a larger difference in temperature between T_0 and T_s .

The variation in temporal variation of radius shown in Figs. 2 and 3 for $\tau \geq .01$ with field liquid properties illustrate the potential impact of the field liquid on bubble growth rate. \dot{R} may be dramatically increased (high ζ or low γ), or decreased (low ζ , high γ) as a result of penetration of the boundary layer into liquid2. This fact could have important implications with regard to the vapor explosion problem.

When the thermal boundary layer reaches the liquid1/liquid2 interface, the radius grows more rapidly for smaller values of γ as shown in Figure 2. A value of γ less than one implies that the thermal diffusivity of liquid2 is smaller than that of liquid1.

This causes the thermal boundary layer to grow more slowly in liquid2 than in liquid1, thus causing temperature gradients to be higher everywhere compared to the infinite medium case ($\gamma=1$). From Equation (17) it can be seen that this leads to an increased bubble growth rate. A reversal of this trend is observed for values of γ greater than 1. Physically, a lower value of γ for a constant value of ζ means that the heat capacity per unit volume, $\rho_2 C_{p2}$ of liquid2 is greater than $\rho_1 C_{p1}$. This implies that a given volume of liquid2 can supply more heat than an equal volume of liquid1. This tends to increase the rate of bubble growth as shown in Figure 2.

Figure 3 shows the effect of varying ζ on bubble growth. Here again the different curves are identical until the thermal boundary layer reaches the bubble wall. Beyond this time, a higher ζ leads to a higher growth rate. A higher value of ζ means a high thermal conductivity for liquid2 compared to liquid1. Temperature gradients within liquid2 are then relatively smaller so that most of the temperature rise takes place within the thin layer of liquid1 surrounding the bubble. The attendant increase in the temperature gradient then increases the growth rate of the bubble. Interpreted physically, a higher thermal conductivity for liquid2 causes a higher heat transfer rate to the bubble, thus increasing the growth rate.

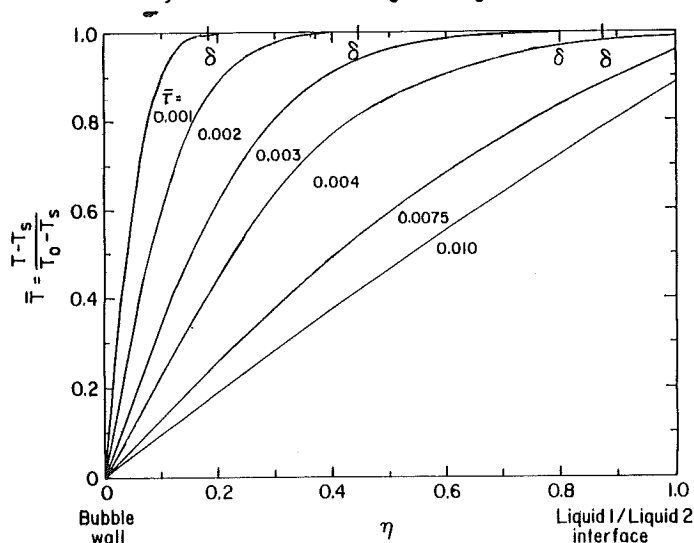


Fig. 5. Temperature profiles within the droplet ($0 < \eta < 1$) at early times for $Ja=10$, $\epsilon=1$, $\gamma=1$ and $\zeta=5$.

Figures 5 and 6 show representative temperature fields in the droplet and ambient liquid at various times. Figure 5 essen-

tially illustrates the evolution of the thermal boundary layer ($\bar{T} > 1$) in the droplet

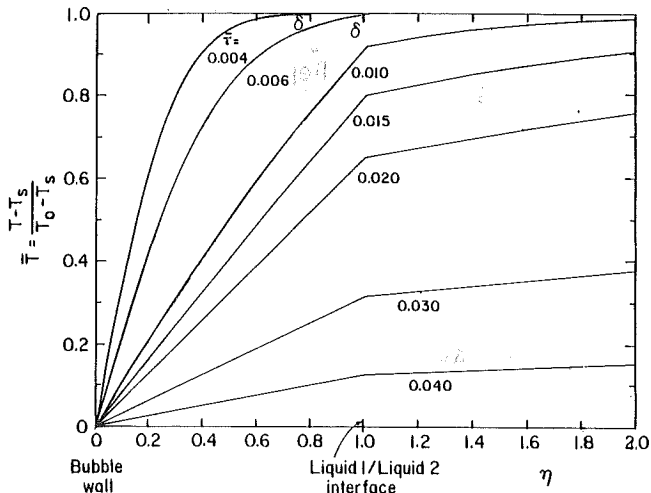


Fig. 6. Temperature profiles within and outside ($\eta > 1$) a droplet at various times for $Ja=10$, $\epsilon=1$, $\gamma=1$ and $\zeta=5$.

($0 < \eta < 1$) at various times. The temperature field here is identical to the temperature field which would be obtained for a bubble growing in an infinite medium of liquid1. At later times (Figure 6) the thermal boundary layer extends into liquid2 ($\bar{T} < 1$ when $\eta > 1$). The field liquid temperature then begins to drop, as expected, thus giving rise to heat transfer between the ambient and liquid1/liquid2 interface. This is manifest by a temperature gradient in the field liquid ($\eta > 1$). For conditions of the calculation appearing in Fig. 6, the liquid1/liquid2 interface temperature gradient in the droplet ($0 < \eta < 1$) is higher than the corresponding temperature gradient in the field liquid ($\eta < 1$). This fact is consistent with Equation 18.

For sufficiently long times, the temperature gradient in liquid1 becomes essentially linear as shown in Fig. 6. This result is consistent with the extreme thinness of the liquid layer surrounding the vapor bubble at these later times (while $0 < \eta < 1$, $S-R \rightarrow 0$ at $\tau \approx .02$). This fact could lead to a simplified analysis for bubble growth which obviates the need to include the full energy equation governing the temperature field in liquid1--Eq. 1--and assumes outright a linear temperature field within the droplet. However, it is clear from the present analysis that the assumption of a linear temperature field in liquid1 could generally lead to serious errors in computed bubble growth rates.

As liquid1 evaporates both the internal vapor bubble and the droplet (as a whole) expand. Evaporation is complete and the solution terminated when $\bar{R} > \bar{S}$ (Figure 1). Figure 7 illustrates the temporal variation of both \bar{S} and \bar{R} for $Ja = 10$ for one representative set of parameters. When the curves describing the evolution of \bar{S} and \bar{R} intersect, the droplet is completely vaporized. The

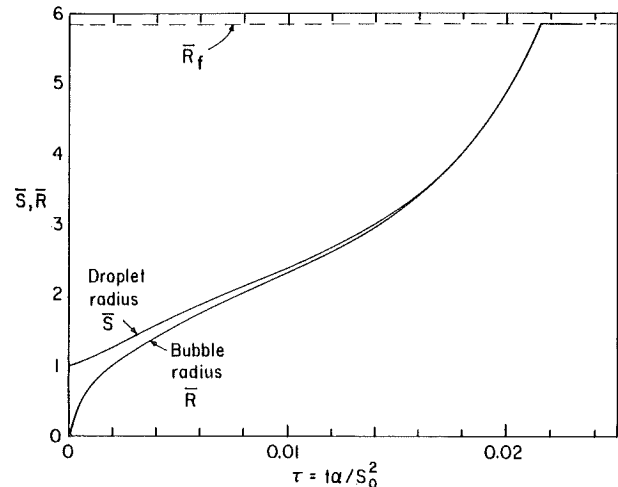


Fig. 7. Relationship between the droplet radius (\bar{S}) and bubble radius (\bar{R}) during growth for $J=10$, $\epsilon=.995$, $\gamma=1$ and $\zeta=5.0$.

size of the final vapor bubble--the point of termination of the solution--is determined from an overall mass balance (Equation 20), and depends on ϵ . The solutions shown in Figures 2 to 4 and have been carried to this bubble size and then terminated.

The temporal variation of bubble radius (e.g., Figs. 2 and 3) will eventually approach the classical asymptotic result

$$R \sim t^n$$

where $n=1/2$ if liquid1 does not completely vaporize beforehand. This fact is illustrated in Fig. 8 where the calculations of Fig. 2 for $\gamma=.2, 1$, and 5 have been re-plotted on a logarithmic scale to more clearly display the slopes involved. As long as the thermal boundary layer remains within the confines of the droplet, the bubble grows as if it were in an infinite medium of liquid1. When the thermal boundary layer penetrates into liquid2, n may be larger or smaller than $1/2$ as shown in Fig. 8. When $\gamma > 1$, the temperature gradient in liquid2 is larger than the corresponding gradient in liquid1. The growth rate decreases compared to the infinite

medium case and $n < 1/2$; the opposite is true when $\gamma < 1$. Eventually, as the thickness of

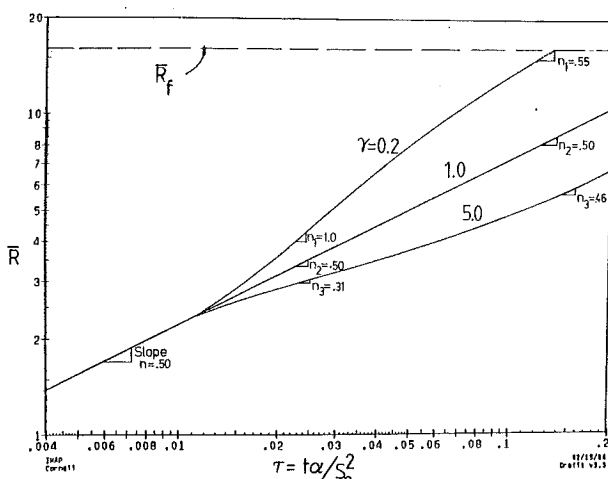


Fig. 8. Variation of bubble radius with time for $Ja=10$, $\zeta=1$, and $\gamma=.2, 1.,$ and 5 , illustrating the change in growth rate as time advances. As $\tau \rightarrow \infty$, $n \rightarrow 1/2$.

the liquid layer becomes very small compared to the thermal boundary layer thickness, the contribution of liquid to the thermal resistance becomes negligible and the temperature field resembles that which would exist for a bubble growing in an infinite medium of liquid 2. As a result, we again have $n \rightarrow 1/2$ as shown in Fig. 8.

CONCLUSIONS

A numerical solution for bubble growth in a suspended volatile liquid droplet immersed in a hot immiscible non-volatile field liquid was obtained which takes into account the temperature and velocity fields both within the droplet and in the ambient liquid. Results showed that the vapor bubble in the droplet grows according to the classical heat transfer growth law corresponding to a bubble in an infinite medium until the thermal boundary layer reaches the liquid 1/liquid 2 interface. Beyond this time, the field liquid influences bubble growth, and the temporal variation of bubble radius deviates from the classical result. Though the growth rate may deviate from the classical growth law as a result of thermal boundary layer penetration into the field liquid, eventually the bubble growth law conforms to the classical result for sufficiently large times.

ACKNOWLEDGEMENTS

This work was supported in part by the National Science Foundation under Grant No. CPE-8106348 (Dr. Robert M. Wellek, Project Monitor), and by the Department of Energy, Office of Basic Energy Sciences -- Engineering Research Program (Dr. Oscar P. Manley, Project Monitor) under Contract No. DE-AC02-83ER13092. This support is gratefully acknowledged.

NOTATION

A, B, C	Coefficients in transformed energy equation defined in equations (25) and (26)
C	Specific heat
h_{fg}^p	Latent heat of vaporization of liquid 1 at T_s
Ja	Jakob number
k	Thermal conductivity
P	Ambient pressure
r^0	Radial coordinate
R	Radius of bubble
\dot{R}	Radial velocity of bubble wall
S	Droplet radius
S^0	Initial droplet radius
t^0	Time
T	Temperature
T_s	Saturated vapor temperature of liquid 1 at P_0
T_0	Homogeneous nucleation temperature of liquid 1 at P_0
V	Velocity

Greek

α	Thermal diffusivity
ϵ	Density ratio $(\rho_1 - \rho_v)/\rho_1$
γ	Diffusivity ratio α_2/α_1
ζ	Conductivity ratio k_2/k_1
η	Transformed radial coordinate
ρ	Density
τ	Transformed time coordinate

Subscripts

1	liquid 1
2	liquid 2
v	vapor 1
k	position level descriptor

Superscripts

n	Time level descriptor
-	Indicates nondimensional quantity

LITERATURE CITED

1. Sideman, S. and Taitel, Y., Direct Contact Heat Transfer with Change of Phase: Evaporation of Drops in an Immiscible Liquid Medium, International Journal of Heat and Mass Transfer, Vol. 7, 1964, pp. 1273-1289.
2. Sideman, S. and Isenberg, J., Direct Contact Heat Transfer with Change of Phase: Bubble Growth in Three Phase Systems, Desalination, Vol. 2, 1967, pp. 207-214.
3. Isenberg, J. and Sideman, S., Direct Contact Heat Transfer with Change of Phase: Bubble Condensation in Immiscible Liquids, International Journal of Heat and Mass Transfer, Vol. 13, 1970, pp. 997-1011.
4. Tochtani, Y., Nakagawa, T., Mori, Y.H. and Komotori, K., Vaporization of Single Liquid Drops in an Immiscible Liquid, Wärme-und Stoffübertragung, Vol. 10, 1977, pp. 71-79.
5. Mokhtarzadeh, M.R. and El-Shirbini, A.A., A Theoretical Analysis of Evaporating Droplets in an Immiscible Liquid, International Journal of Heat and Mass Transfer, Vol. 22, 1979, pp. 27-38.
6. Avedisian, C.T., "Effect of Pressure on Bubble Growth within Liquid Droplets at the Superheat Limit", Journal of Heat Transfer, Vol. 104, No. 4, 1982, pp. 750-757.
7. Scriven, L.E., On the Dynamics of Phase Growth, Chem. Eng. Sci., Vol. 10, 1959, pp. 1-13.
8. Avedisian, C.T., "The Homogeneous Nucleation Limits of Liquids", Journal of Physical and Chemical Reference Data, to appear (1984).
9. Duda, J.L., Malone, M.F., Notter, R.H. and Vrentas, J.S., Analysis of Two-dimensional Diffusion Controlled Moving Boundary Problems, International Journal of Heat and Mass Transfer, Vol. 18, 1975, pp. 901-910.
10. Saitoh, T., Numerical Method for Multi Dimensional Freezing Problems in Arbitrary Domains, Journal of Heat Transfer, Vol. 100, 1978, pp. 294-299.
11. Heurtault, S., Badie, J.M., Rouanet, A. and Arnand, G., Solidification de spheres Liquides Surchauffees a Caracteristiques Physiques Variables, International Journal of Heat and Mass Transfer, Vol. 25, 1982, pp. 1671-1676.
12. Moore, F.E. and Bayazitoglu, Y., Melting within a Spherical Enclosure, Journal of Heat Transfer, Vol. 104, 1982, pp. 19-23.
13. Prusa, J., and Yao, L.S., Melting Around a Horizontal Heated Cylinder: Perturbation and Numerical Solutions for Constant Heat Flux Boundary Condition, Paper No. 83-HT-18, 21st. ASME/AIChE National Heat Transfer Conference, Seattle, July 24-28, 1983.
14. Suresh, K., Vaporization of Superheated Liquid Droplets, M.S. Thesis, Cornell University (1984).